

MAGNETIC DOMAIN BEHAVIOR AND INTERPRETATION IN APOLLO SAMPLES. B. E. Strauss^{1,2} and S. M. Tikoo³, ¹Materials Science and Engineering Division, National Institute of Standards and Technology, 100 Bureau Drive, Gaithersburg, MD 20899, ²NASA Goddard Space Flight Center, Greenbelt, MD 20771 (beck.strauss@nasa.gov), ³Department of Geophysics, Stanford University, Stanford, CA 94305.

Introduction: In the fifty years following the Apollo missions, paleomagnetic analyses of lunar rocks have revealed evidence for ancient magnetic fields with intensities sometimes comparable to that of the Earth's present-day field. Magnetic characterization provides information about the metallic mineralogy of lunar rocks based on their behavior in applied magnetic fields and is critical for the efficient selection and use of Apollo samples for paleomagnetic study. Although terrestrial magnetic minerals are generally well-characterized and the disciplines of rock and paleomagnetism on Earth have made major advances in understandings of magnetic domain theory and grain-scale processes, lunar rock magnetism lags behind. The magnetic recording capabilities of the ≈ 20 Apollo samples analyzed with modern paleomagnetic methods vary widely and the underlying mineralogical mechanisms have yet to be explained.

We present a case study of Apollo 12 basalts 12008, 12009, and 12015, with two aims: (1) to address fundamental questions about the magnetic mineralogy of lunar material by incorporating more nuanced discussions of domain state and grain size now considered standard for terrestrial studies, and (2) to improve our understanding of the relationship between mineralogy and magnetic fidelity in lunar rocks.

Lunar Magnetic Mineralogy: While remanent magnetization in terrestrial rocks is typically carried by iron oxides, the most common carriers of magnetization in lunar rocks are iron minerals. Early studies of Apollo samples indicated that their ferromagnetic mineralogy was dominated by metallic iron (Fe^0) [1]. This assessment was later expanded to include both iron metal and iron alloys with nickel, cobalt, and other trace contaminants, and the most commonly found form was recognized as kamacite (α -(Fe,Ni)) [2], [3]. In the past decade, the development of improved paleomagnetic methods for the assessment of magnetic fidelity in lunar material have been accompanied by more detailed analyses of ferromagnetic carriers. Nonmagnetic analyses have enabled finer-scale evaluation of Fe-Ni compositions, including differentiation of kamacite and martensite (α_2 -(Fe,Ni)) by Ni mass fraction ($< 5\%$ and $5\% \leq \text{Ni} < 25\%$ respectively) [4].

All lunar paleomagnetism studies since 2009 have identified kamacite, martensite, and/or metallic iron as the main carriers of magnetization. However, compared to terrestrial minerals like magnetite and hematite, the magnetic behavior of these iron minerals is not

as well-characterized, and the role of properties like Fe:Ni ratio, grain size, cooling history, and other parameters in determining the magnetic properties of a given rock sample is not fully understood. In addition, several studies have pointed to association of Fe-Ni grains with other minerals like schreibersite ($(\text{Fe},\text{Ni})_3\text{P}$), cohenite (Fe_3C), and troilite ($\text{Fe}_{(1-x)}\text{S}$, $x = 0$ to 0.02), which is antiferromagnetic but has been suggested to contribute to remanence [3], [5].

Advances in Domain Theory: Modern approaches to both experimental methods and the strategies used to interpret magnetic characterization data in terrestrial materials can, and must, be used to advance astromaterial magnetism past simple expressions of bulk mineralogy and toward more complex explorations of grain- and sub-grain-scale dynamics.

Experimental methods. A variety of magnetic characterization experiments have been conducted on lunar samples since the Apollo era, producing a body of publications that establish a baseline for expressions of lunar magnetic mineralogy. More than 80 Apollo rock and soil samples have been subject to hysteresis experiments (Figure 1), often accompanied by bulk magnetic susceptibility determinations. Several recent studies [6]–[8] have supplemented hysteresis loops with first-order reversal curves (FORCs), which provide further insight into distributions of coercivities and magnetic interactions between populations of particles.

Improvements to interpretation. Dunlop-Day plots [9] have frequently been used to evaluate the magnetic domain state (and thus grain size) of magnetic min-

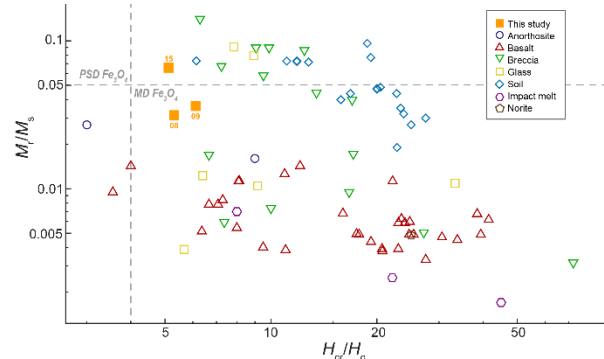


Figure 1. Day plot [9] of hysteresis parameters for Apollo samples, modified from [12]. Remanent coercivity (H_{cr}) divided by coercive force (H_c) for each sample is plotted against magnitude of saturation remanent magnetization (M_r) divided by magnitude of saturation magnetization (M_s). Data from previous studies are plotted as open shapes. Magnetite domain state regions shown in gray.

als, including those found in lunar samples [8], [10], based on their hysteresis behavior. However, current best practices in terrestrial rock magnetism [11] discourage the use of these plots for such interpretation, as their inherent ambiguity can inadvertently encourage erroneous conclusions. The magnetic grain size parameters developed through Day's work were defined for compositionally pure euhedral magnetite (Fe_3O_4), whose magnetic behavior is completely distinct from that of Fe-Ni minerals with respect to everything from permeability to fidelity.

Nevertheless, a generic Day plot may be used constructively to compare the magnetic properties of large groups of samples without ascribing strict grain size parameters based on bulk magnetic behavior, and theoretical Day plots for particular iron minerals may be constructed and later grounded experimentally through laboratory analyses. While this would not produce a simple tool for conclusive determination of domain state in natural rocks, it would represent a substantial improvement to the current understanding of iron minerals in the context of paleomagnetic applications.

Case Study: Mare basalt samples 12008, 12009, and 12015 were collected in the southeastern region of Oceanus Procellarum during the Apollo 12 mission. All three are fine-grained olivine vitrophyres that exhibit excellent magnetic fidelity (paleointensity fidelity thresholds $\approx 4\text{-}7 \mu\text{T}$) and multidomain (MD) behavior in hysteresis experiments [12]. Comparison of these results to previously published literature illustrates that the relationship between these properties is not simple. For example, samples 12008, 12009, and 12015 provide more restrictive paleointensity constraints than more crystalline basalts, such as the porphyritic basalt portion of sample 12017 ($\approx 37 \mu\text{T}$ [4], [13]), medium-grained basalt 15016 ($\approx 37 \mu\text{T}$ [6]), and fine-grained basalt 15556 ($\approx 75 \mu\text{T}$ [6]). The unreliable remanence behavior of the latter basalts has been attributed in part to their relatively high fractions of MD grains compared to mare basalts with more readily retrieved paleointensities [6], [10], [14], [15]. However, glassy rocks like sample 15597, a rapidly cooled vitrophyric pigeonite basalt, and the glass spatter coating of sample 12017 both exhibit MD magnetic behavior and $\approx 7 \mu\text{T}$ paleointensity fidelity thresholds [4], [13].

This range in fidelity limits has been attributed to a variety of sources, including magnetic anisotropy, composition, and grain size. Figure 1 shows a modified Day plot of hysteresis parameters for samples collected during the Apollo missions, adding the three samples from this study in orange. Bulk rock types are distinguished by point shape; although some broad trends are apparent (e.g., relatively low M_r/M_s for basalts

compared to other rock types), this initial categorization clearly does not explain the range of paleomagnetic recording behaviors reported in the sample suite.

Non-magnetic analyses offer other possible explanations for remanence behavior, including possible incongruities between petrographically observed grain size and the grain sizes typically inferred from magnetic measurements. Electron microprobe characterization of sample 15597 identified three distinct populations of constituent kamacite and martensite based on both grain size (ranging from ≈ 1 to $20 \mu\text{m}$) and association with other minerals [1], [4]. Samples 12008, 12009, and 12015 contain both submicrometer metallic grains too small for conclusive identification and larger martensite grains whose MD behavior could dominate simple hysteresis experiments. Troctolite 76535 exhibits similar hysteresis parameters but its magnetic grains have been reported to be pseudo-single domain in size [16]. Magnetic anisotropy may further complicate efforts to analyze samples initially magnetized in weak paleofields [4], [6]. Perhaps most critically, recent work in terrestrial micromagnetics has shown that the domain size model itself may be an oversimplification [17]. In this study, we explore the Apollo magnetism literature to evaluate possible contributors to remanence behavior and assess whether iron mineral grain size is, in fact, the dominant controller of paleomagnetic fidelity in lunar rocks.

Acknowledgments: We thank the Curation and Analysis Planning Team for Extraterrestrial Materials (CAPTEM) for sample allocation.

References: [1] Fuller M. (1974) *Rev. Geophys. Sp. Phys.*, 12, 23–70. [2] Garrick-Bethell I. and Weiss B. P. (2010) *Earth Planet. Sci. Lett.*, 294, 1–7. [3] Rochette P. et al. (2010) *Earth Planet. Sci. Lett.*, 292, 383–391. [4] Tikoo S. M. et al. (2014) *Earth Planet. Sci. Lett.*, 404, 89–97. [5] Kletetschka G. and Wieczorek M. A. (2017) *Phys. Earth Planet. Inter.*, 272, 44–49. [6] Tikoo S. M. et al. (2012) *Earth Planet. Sci. Lett.*, 337, 93–103. [7] Tikoo S. M. et al. (2017) *Sci. Adv.*, 3, 1–10. [8] Mighani S. et al. (2020) *Sci. Adv.*, 6, 1–8. [9] Day R. et al. (1977), *Phys. Earth Planet. Inter.*, 13, 260–267. [10] Cournède C. et al. (2012) *Earth Planet. Sci. Lett.*, 331–332, 31–42. [11] Roberts, A. P. et al. (2018) *J. Geophys. Res. Solid Earth*, 123, 2618–2644. [12] Strauss B. E. et al. (2021) *J. Geophys. Res. Planets*, in press. [13] Buz J. et al. (2015) *J. Geophys. Res. Planets*, 120, 1720–1735. [14] Shea E. K. et al. (2012) *Science*, 335, 453–456. [15] Suavet C. (2013) *Proc. Natl. Acad. Sci.*, 110, 8453–8458. [16] Garrick-Bethell I. et al. (2009) *Science*, 323, 356–359. [17] Roberts A. P. et al. (2017) *J. Geophys. Res. Solid Earth*, 122, 9534–9558.